C. R. Chimie 15 (2012) 336–345

Contents lists available at SciVerse ScienceDirect

Comptes Rendus Chimie

www.sciencedirect.com

Full paper/Mémoire

Solution studies of tris(2-benzylaminoethyl)amine complexes of zinc(II) and copper(II): The catalytic hydrolysis of toxic organophosphate

Gaber A.M. Mersal [a,c,*], Mohamed M. Ibrahim [b,c]

[a] Chemistry Department, Faculty of Science, South Valley University, 83523 Qena, Egypt
[b] Chemistry Department, Faculty of Science, Kafr El-Sheikh University, 33516 Kafr El-sheikh, Egypt
[c] Chemistry Department, Faculty of Science, Taif University, 888 Taif, Saudi Arabia

ARTICLE INFO

Article history:
Received 3 August 2011
Accepted after revision 24 October 2011
Available online 4 January 2012

Keywords:
Zinc(II)
Copper(II)
Tris(2-benzylaminoethyl)amine
^{1}H NMR and UV-visible titrations
Kinetic
Phosphate hydrolysis

ABSTRACT

Solution studies of the tetradentate ligand tris(2-benzylaminoethyl)amine, BzTren with both zinc(II) and copper(II) salts were investigated in aqueous methanol (33% *v/v*) by means of ^{1}H NMR, potentiometric, and UV-visible titrations as well as cyclic voltammetry. Subsequently, their zinc(II) and copper(II) complexes $[BzTren\text{-}M(OH_2)]^{2+}$ **1** and **2** ($M^{2+} = Zn^{2+}$ and Cu^{2+}) were synthesized and fully characterized by using FT-IR spectroscopy, elemental analysis, and thermal analysis. Complexes **1** and **2** are investigated kinetically for the catalytic hydrolysis of the toxic organophosphate parathion at 50 °C in aqueous methanol (33%, *v/v*). The kinetic results indicate that copper(II) complex **2** is more active than zinc(II) complex **1**, presumably a reflection of the effective electron-withdrawing as well as the greatest electrophilicity of copper(II) ion.

1. Introduction

The development of metal-containing catalysts for the rapid hydrolysis of toxic organophosphorus triesters is of a fundamental and practical interest since these compounds appear from day-to-day applications as pesticides and potent chemical warfare agents [1]. Recently, many hydrolytic metalloenzyme models have been designed and studied to account for or mimic the function played by the central metal ions [2–8].

There has been a considerable amount of research conducted on the transition metal-substituted metalloproteins [9]. The primary reason for the substitution, for example cobalt, copper, nickel, or iron for zinc, is the paramagnetism of these transition metals and their sensitivities to changes in their coordination geometries that appear in their visible absorption spectra. With this aim, various polydentate ligands containing three or four functional donors have been synthesized [10–16]. The use of tripod-like ligand, tris(2-benzylaminoethyl)amine, BzTren (Scheme 1) with hydrophobic benzene rings can provide protected 'pockets' for metal ions and was also suitable for the synthesis of biomimetic coordination compounds having *phosphatase* activity [17,18].

With the aim of mimicking the key features of the nature of metal(II) centers in these metalloenzymes, our target is:

- synthesis of Zn^{2+} and Cu^{2+} complexes derived from the tetradentate ligand BzTren;
- analysis and characterization of the obtained compounds in the solid state using FT-IR spectroscopy, elemental analysis, and thermal analysis;
- solution structural studies of zinc(II)/copper(II)-ligand interactions for determining the stoichiometry and the pK_a value of the coordinated water molecule using ^{1}H NMR and UV-visible spectroscopies, as well as cyclic voltammetry (CV);
- application of these obtained metal complexes towards the hydrolysis of the toxic organophosphate parathion (Scheme 2).

* Corresponding author.
E-mail address: gamersal@yahoo.com (Gaber A.M. Mersal).

1631-0748/$ – see front matter
doi:10.1016/j.crci.2011.10.012

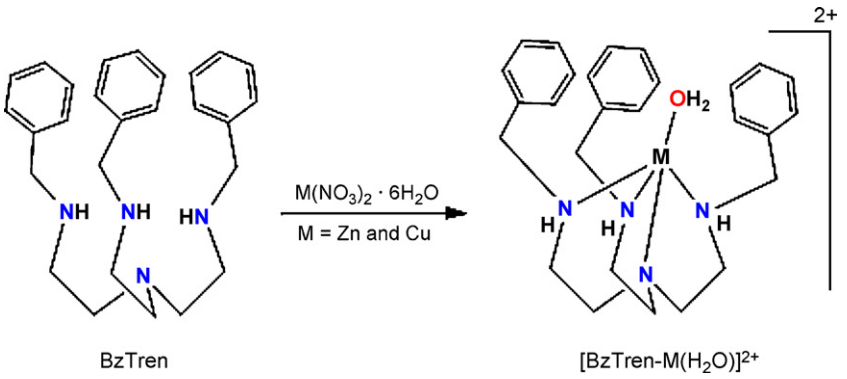

Scheme 1. The tripodal ligand BxTren and its metal complexes.

2. Experimental

2.1. Materials and general methods

The ligand tris(2-benzylaminoethyl)amine, BzTren, has previously been synthesized and described [17]. The IR absorption spectra were recorded using FT-IR Prestige-21 Shimadzu, in the range of 400–4000 cm^{-1}. The ^1H NMR measurements were recorded by using Varian 400-MR. The conductivity measurements were carried out using Equiptronics digital conductivity meter model JENWAY 4070 type at room temperature for (1×10^{-3} M) solutions. All UV-visible measurements were recorded by UV-1650pc Shimadzu.

2.2. Syntheses of the metal complexes

2.2.1. *[BzTren-Zn(OH$_2$)](NO$_3$)$_2$* **1**

A solution of 89 mg (0.30 mmol) of $Zn(NO_3)_2 \cdot 6H_2O$, dissolved in anhydrous methanol (5 ml) was added to a solution of BzTren, made up from (182 mg, 0.3 mmol) of the acid form BzTren·3HNO_3 and 3.6 ml (0.9 mmol) of CH_3ONa (0.25 mM) in 5 ml of anhydrous methanol. The resulting solution was stirred for another 3 h at room temperature and then evaporated to dryness at 40 °C. The residue was extracted with CH_2Cl_2, filtered, and evaporated to dryness again. Recrystallization from methanol yielded 158 mg (84%) of **1** as colorless crystals, Anal. Calc. for $C_{27}H_{38}N_6O_7Zn$ (622.21): C, 51.96; H, 6.14; N, 13.47; Zn, 10.48. Found: C, 51.38; H, 6.21; N, 13.32; Zn, 10.55%. Conductivity (Ω cm, mole^{-1}: 122. IR (KBr): ν(OH) 3377; ν(NH) 3180; ν(CH_{aliph}) 2934; ν(CH_{arom}) 1001, 743, 702; ν(NO) 1390; ν(M-N) 439. ^1H NMR (CD_3OD, 298 K, TMS: 7.46–7.43 (m, 15H,–C_6H_5–), 3.37(s, 6H, C_6H_5–CH_2–), 2.82 (t, 6H,–$^{\alpha}CH_2$) and 2.75 ppm (t, 6H,–$^{\beta}CH_2$–).

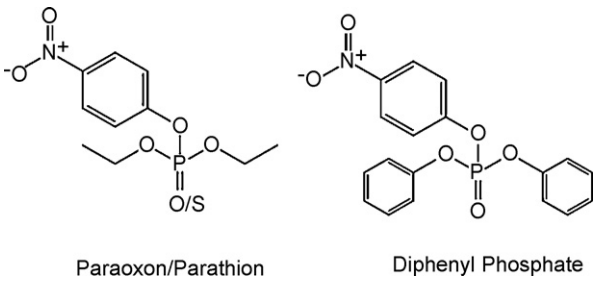

Scheme 2. The toxic organophosphate.

2.2.2. *[BzTren-Cu(OH$_2$)](NO$_3$)$_2$ .H$_2$O* **2**

The copper(II) complex **2** was prepared in a fashion similar to zinc(II) complex **1**: 72 mg (0.30 mmol) of $Cu(NO_3)_2 \cdot 3H_2O$, 182 mg (0.3 mmol) of BzTren·3HNO_3, and 3.6 ml (0.9 mmol) of CH_3ONa (25 mM). Yield: 152 mg (79%) of **2** as blue crystals, Anal. Calc. for $C_{27}H_{40}N_6O_8Cu$ (639.19): C, 50.65; H, 6.29; N, 13.13; Cu, 9.93. Found: C, 51.21; H, 6.17; N, 13.22; Cu, 10.05%. Conductivity (Ω cm, mole^{-1}: 124. IR (KBr):): ν(OH) 3375; ν(NH) 3183; ν(CH_{aliph}) 2934; ν(CH_{arom}) 1000, 741, 701; ν(NO) 1388; ν(M-N) 443.

2.2.3. *[(BzTren)-Zn-OP(S)(OC$_2$H$_5$)$_2$)](NO$_3$)* **3**

Complex **3** was prepared by mixing a solution of [BzTren-Zn(OH$_2$)](NO$_3$)$_2$ **1** (310 mg, 0.5 mmol) in abs. methanol (10 ml) and the triester parathion (115 μl, 0.5 mmol) in abs. methanol (10 ml). The reaction mixture was stirred for 4 h at pH = 9.3 and 75 °C. On cooling, complex **3** was precipitated as white needles. CH_3CN (50%, *v/v*). Yield: 272 mg (77%). Anal. Calcd. for $C_{31}H_{46}N_5O_6SZnP$ (713.15): Calc.: C, 52.21; H, 6.51; N, 9.82; S, 4.50; Zn, 9.17. Found: C, 52.04; H, 6.62; N, 9.29; S, 4.43; Zn, 9.22%. Conductivity (Ω cm, mole^{-1}: 113. ^1H NMR, δ_H (DMSO-d_6): 7.48–7.42 (m, 15H, C_6H_5–), 3.79 (q, 4H, O–CH_2–), 3.38 (s, 6H, C_6H_5–CH_2–), 2.80 (t, 6H,–$^{\alpha}CH_2$), 2.76 (t, 6H,–$^{\beta}CH_2$–), and 1.11 ppm (t, 6H, –CH_3). IR (KBr): ν(OH) 3345; ν(NH) 3182; ν(CH_{aliph}) 2936; ν(P = S) 1250; ν(P–O–C), ν(P–S) 1138 and 1129 1129; ν(CH_{arom}) 999, 743, 702; ν(NO) 1383; ν(M–N) 444 cm^{-1}.

2.3. Solution studies

2.3.1. *^1H NMR measurements*

To investigate the coordination behavior toward zinc ions, ^1H NMR analyses of the nature of BenzTren/Zn^{2+} binding in CD_3OD:D_2O (33%, *v/v*) and *I* = 0.1 M $NaNO_3$ were undertaken as a function of pD and at different zinc-to-ligand ratios. The chemical shifts are reported relative to the resonance signal of sodium 2,2-dimethyl-2-silapentane-5-sulfonate (DSS) as an internal standard signals. The pD was adjusted with concentrated NaOD and DNO_3, so that the effect of dilution could be neglected.

2.3.2. Potentiometric pH titration

Potentiometric titrations were carried out at 25 ± 0.2 °C with a TOA AUT-501 automatic titrator connected to a TOA ABT-511 automatic burette with a combined glass electrode. Aqueous methanolic solution (33%, *v/v*) of 1.0 mM of BzTren in the absence and in the presence of equivalent Cu^{2+} ion were titrated with 0.1 M NaOH aqueous solution. Although a correction was not made to compensate for the methanol–water liquid junction potential, a correction of 0.136 pH units can be subtracted from the measured pH readings as suggested by Bates et al. [20] to enable a comparison to be made with measurements in aqueous solution. Equilibrium constants were calculated using the program BEST [21] and species distributions were calculated using the program SPE [21].

2.3.3. Cyclic voltammetry

The electrochemical behavior of the Ligand BzTren and its complexes **1** and **2** were studied using CV and square wave voltammetry (SWV) using Auto lab potentiostat PGSTAT 302 (Eco Chemie, Utrecht, The Netherlands) driven by the General Purpose Electrochemical Systems data processing software (GPES, software version 4.9, Eco Chemie). The electrochemical cell used in this work contains three electrodes; platinum wire was used as a working electrode, SCE as a reference electrode, and a platinum wire was used as a counter electrode.

2.4. Thermal analysis

Thermogravimetric (TG) and differential scanning colorimetric (DSC) analyses of complexes **1**, **2**, and **3** were performed on Netzsch STA 449F3 with system interface device. All the samples were placed in alumina crucibles. Experiments were performed using sample sizes of 6.0 ± 0.3 mg. All the experiments were conducted under nitrogen as the purge gas with a flow rate of 50 ml/min. The range of the temperature studied was from 30 to 1000 °C, at a heating rate of 10 °C/min.

2.5. Kinetic studies for the hydrolysis reactions of parathion

The hydrolysis rate of parathion, DENTP (4×10^{-5} M) in aqueous methanol (33%, *v/v*) at $I = 0.1$ M $NaNO_3$ by using the model complexes **1** and **2** (1.0×10^{-3} M) was measured by recording the increase in 400 nm absorption of the released yellow *p*-nitrophenolate as a hydrolyzed product [17,18]. The measurements of the hydrolysis reactions were carried out at 50.0 ± 0.2 °C. The catalytic reaction was initiated by rapid injection of a THF solution containing 60 mL (2.0 mM) of the toxic phosphate parathion into 3.0 mL of 1.0 mM metal complex solution. Reaction rates are corrected by blank experiments which were made up similarly but without the presence of metal complexes. The pseudo-first-order rate constants, k_{obs}, were obtained from the plot of $\ln(A_\infty/A_\infty - A_t)$ *versus* time.

3. Results and discussion

3.1. Characterization of the model complexes 1–3

The synthesis of the aqua metal complexes [BzTren-$M(OH_2)](NO_3)_2$ (M = Zn **1** and Cu **2**) were carried out in absolute methanol by treating the ligand BzTren with equimolar amounts of the corresponding nitrate salts under anaerobic conditions. The chemical analysis and some physical properties of the isolated pure complexes are listed in Tables 1 and 2. The analytical results demonstrate that all the complexes have (1:1) metal: ligand stoichiometry. The microcrystalline complexes are stable as solids or in solution under the atmospheric conditions. All the investigated complexes behave as 1:2 electrolytes with molar conductance values rang of 113–

Table 1
The computed protonation constants (pK_a) of the ligand **BzTren**, stability constants ($\log K_{st}$), and deprotonation constants (pK_a) of zinc(II) and copper(II) complexes.

Compound	pK_{a1}	pK_{a2}	pK_{a3}	$\log K_{st}$	$pK_a(H_2O)$
BzTren[a]	6.83	8.40	9.39		
$[BzTren\text{-}Zn(OH_2)]^{2+}$ **1**				10.02 [18]	9.61 [18]
$[BzTren\text{-}Cu(OH_2)]^{2+}$ **2**				13.45	8.72

[a] Data was obtained from the ^1H NMR measurements.

Table 2
Thermogravimetric and colorimetric (TG-DSC) data of complexes **1** and **2**.

Complex	Steps	Temp. range (K)	DTG (K)	Peak nature	Mass loss (%) Found (Calc.)	Decomposition Species	Residua
1	1st	327–469	395	Endo	3.08 (2.89)	Coordinated H_2O	$[BzTren\text{-}Zn](NO_3)_2$
	2nd	546–746	592	Endo	61.29 (60.70)	$Et_3N + 3\,C_6H_6 + 1.5\,N_2$	$Zn(NO_3)_2 + C_2H_2$
	3rd	749–941	808	Endo	20.33 (19.93)	$NO + NO_2$	ZnC_2
2	1st	322–383	359	Endo	2.72 (2.81)	Hydrated H_2O	$[BzTren\text{-}Cu(H_2O)](NO_3)_2$
	2nd	383–459	424	Endo	2.87 (2.81)	Coordinated H_2O	$[BzTren\text{-}Cu](NO_3)_2$
	3rd	463–691	502	Endo	58.52 (60.81)	$Et_3N + 3\,C_6H_6 + 1.5\,N_2$	$Cu(NO_3)_2 + C_2H_2$
	4th	712–1111	884	Endo	20.94 (19.93)	$NO + NO_2$	CuC_2

122 Ω^{-1} cm^2 mol^{-1} suggesting that the NO_3^- ions are not bound directly to the central metal ion in solution.

Table 2 lists the observed IR frequencies and band assignments of the ligand BzTren and their aqua complexes **1** and **2**. The IR spectrum of the ligand shows band at 3188 cm^{-1}, which was assigned as ν(NH) absorptions. This band was shifted down field upon complexation with metal ions: 3180, 3183, and 3182 for complexes **1**, **2**, and **3**, respectively. They all exhibit ν(NO) absorption bands of the nitrate anion at 1390, 1388, and 1383 cm^{-1} for complexes **1**, **2**, and **3**, respectively. The recognition and coordination of diethylthiophosphate ($DETP^-$) in $[(BzTren)\text{-}Zn\text{-}OP(S)(OC_2H_5)_2)](NO_3)$ **3** was possible by the reaction of aqua zinc(II) complex **1** with an equivalent amount of the deprotonated form of diethylthiophosphate in water. It was isolated analytically pure with a good yield. Its chemical characterization also showed absorption of 1250 cm^{-1} (s, P = S), 1138 and 1129 cm^{-1} (s, P–S), and 1218 cm^{-1} (s, P–O–C), which are typical characterization bands of coordinated phosphate to metal complexes [18b]. Complexes **1** and **2** as water-containing compounds showed broad bands in the 3440–3470 cm^{-1} region, which are characteristics of ν(OH) absorption. Additionally, the four complexes all appeared weak bands at $\approx$ 439, 443, and 444 cm^{-1}, which suggested the existence of M–N bond.

3.2. ^{1}H NMR titration of the ligand BzTren and its zinc complex species

To get a better insight into the zinc(II) complex species formed in BzTren/Zn^{2+} system, ^{1}H NMR studies were carried out in CD_3OD–D_2O (33%, *v/v*) at different zinc-to-ligand ratios ($R = [Zn^{2+}]_o/[BzTren]_o = 0$, 0.5, and 1.0) as a function of pD. Fig. 1 shows the ^{1}H NMR spectra of the triplet methylene proton resonances (α and β). As shown in Fig. 1 (left, $R = 0.0$), the triplet methylene proton signals of the free ligand showed large upfield shifts upon increasing the pD value between 8.0 and 10.0. This large upfield shifts resulted from the stepwise deprotonation of the protonated secondary amino groups. From the computer fit of the pD profile, we were able to evaluate the chemical shifts of the two non-equivalent methylene protons (α and β) in the following species: BzTren, $HBzTren^+$, $H_2BzTren^{2+}$, and $H_3BzTren^{3+}$. The computed pK_a values of the secondary amino groups were determined to be 9.39, 8.40, and 6.83 (Table 1). These obtained pK_a values were in good agreement to those obtained by potentiometric titration [17]. The fourth pK_a does not seem to have been reported, presumably because it is very low: we found that the chemical shifts did not deviate significantly from those of $H_3BzTren^{3+}$ until *ca.* pD = 1.0, suggesting that the pK_a is in the region of 0.0. The spectral

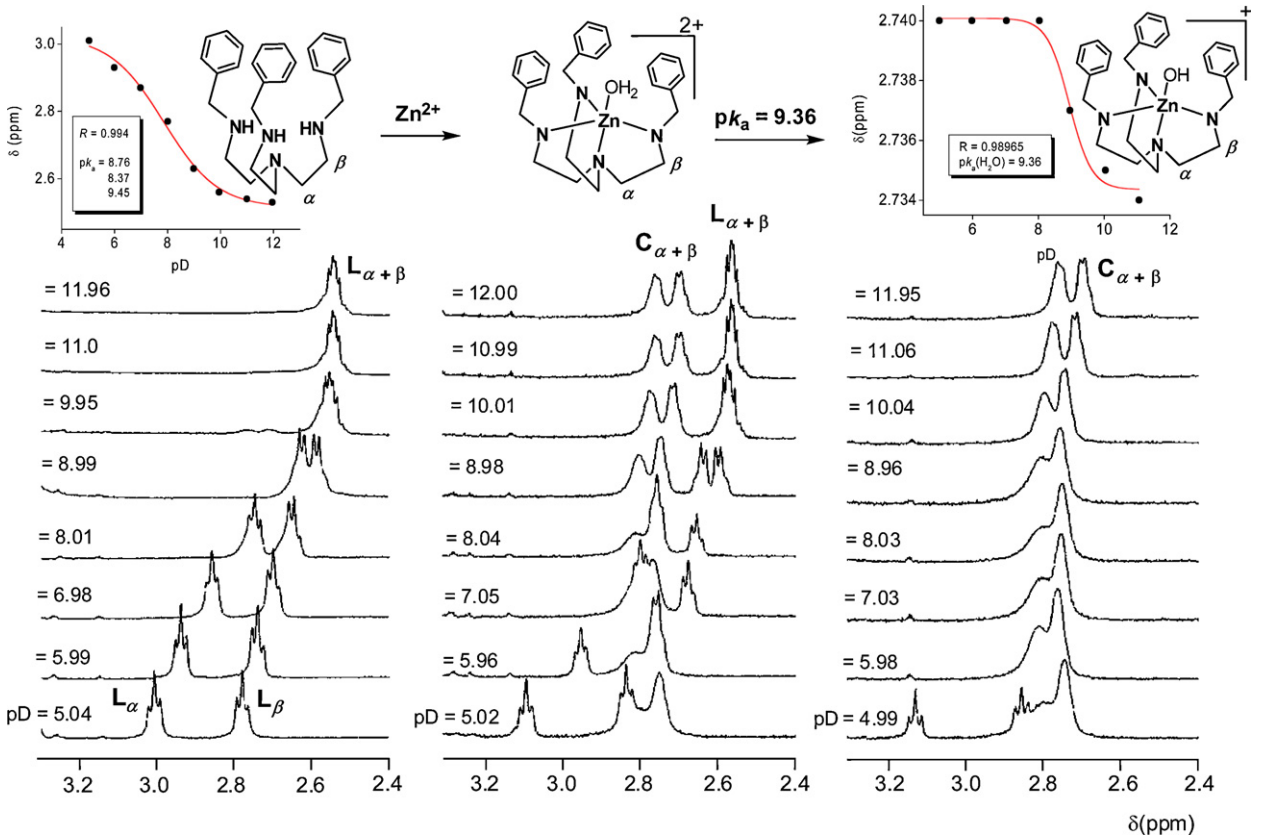

Fig. 1. ^{1}H NMR titration of the ligand BzTren (2.0×10^{-3} M) as a function of pD at different ratios ($R = [Zn^{2+}]_o/[BzTren]_o$): $R = 0.0$ (left), $R = 0.5$ (middle), and $R = 1.0$ (right) in CD_3OD:D_2O (33%, *v/v*) at $I = 0.1$ M KNO_3 and 25 °C.

lines of the ligand itself were consistently sharp and of approximately the same height, this confirms that the exchange between the various protonated species is rapid on the NMR time-scale.

In the case of 1:2 zinc(II)-to-BzTren ratio (Fig. 1, middle), two clearly distinguishable sets of peaks were appeared (kinetically stable species with equal ratio), which were assigned as free and complexed form of the ligand. The peaks of the free ligand shifted upfield, indicating the deprotonation of the ligand donor atoms and the chemical shifts became constant at pD 9.0, whereas the peaks of the complexed form showed no change in the chemical shift in the pD between 3–8 intervals. Between pD 4 and 6, the chemical shifts of the triplet and singlet methylene protons showed 0.1 ppm upfield shift. This shift was also found in the case of methylene protons of the ligand system in the same pD region but with much larger magnitude. This indicates that there is a possibility for the coordination of the tertiary amine nitrogen.

The observed ^{1}H NMR signals of the methylene protons of the zinc compound **1** species at $R = 1$ was shown in Fig. 1 (right). At pD 5, the observed signals show that the zinc complex and free ligand coexist in the solution. At pD 6, the triplet methylene proton signals of the free ligand disappeared whereas the triplet signals related to the zinc complex species are only seen. The chemical shift of these CH_2 proton signals were constant between pD 5.9 and 8.9, which means the formation of 1:1 compound $[BzTren\text{-}Zn(OH_2)]^{2+}$. Further upfield chemical shift (Fig. 2 (right)) indicates a sigmoidal change in the pH range 9 to 10, which corresponds to a change from $[BzTrenZn(H_2O)]^{2+}$ to $[BzTren(OH)]^{+}$. The obtained pK_a value (9.36 ± 0.1) is in very good agreement with the pK_a value (9.63) obtained from potentiometric titration [17]. The 0.4–0.6 ppm downfield shifts for zinc-bound H_2O/OH compared with the chemical shift of the free water resulted from the decrease in electron density by the coordination to zinc and is mainly attributed to the effect of Lewis acidity of zinc. The *ca.* 0.2 ppm upfield shift for zinc–bound OH, compared with the chemical shift of zinc-bound H_2O, resulted from the increase of electron density by the deprotonation of zinc-bound H_2O.

3.3. Copper(II) complexation constant of BzTren

The obtained stability constants, $\log K_{st}$ and deprotonation constants, $pK_a(H_2O)$ of copper(II) complex are listed in Table 1. The first buffer region until $a = 3$ is ascribed to the loss of three protons from the primary amino groups. When the bridgehead nitrogen was considered in the calculation, a worse fitting was obtained. The second buffer region at $3 < a < 4$ represents the removal of a proton from the copper(II)-bound water molecule at the fifth site with a pK_a value of 8.93. Fig. 2 shows the species distribution curves of the ligand BzTren containing both zinc(II) and copper(II) species. The potentiometric data also indicated that BzTren forms a more stable complex with Cu(II) ($\log K_s = 13.45$) than does Zn(II) ($\log K_s = 10.02$ [17]). The lowering in $pK_a(H_2O)$ value of complex **2** (8.72) compared to complex **1** (9.63) is presumably a reflection of the effective the greatest electrophilicity of copper(II) ion.

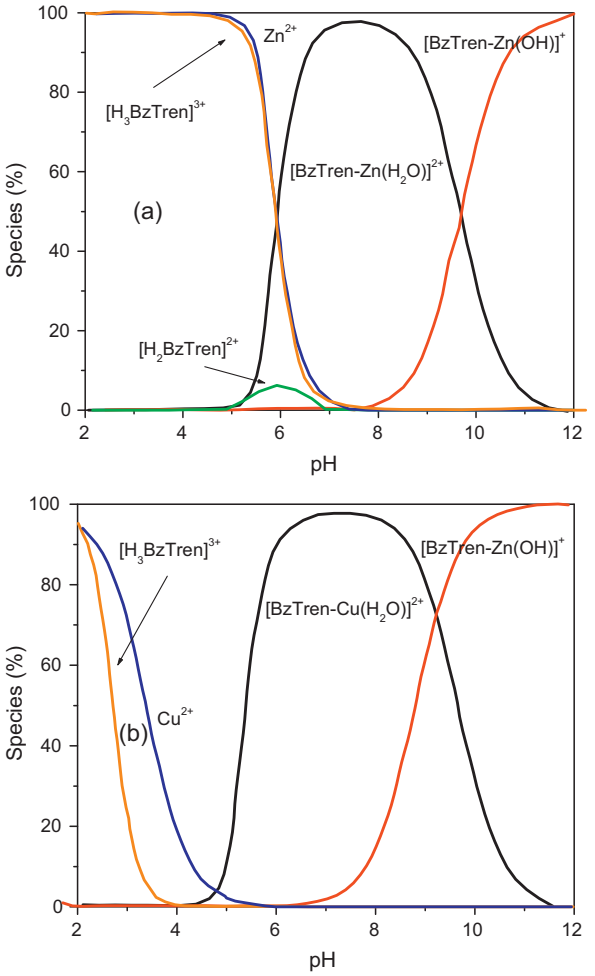

Fig. 2. Species distribution curves of 1.0×10^{-3} M BzTren and (a) 1.0×10^{-3} M Zn^{2+}; (b) 1.0×10^{-3} M Cu^{2+} in aqueous MeOH (33% v/v) at $I = 0.1$ M $NaNO_3$ and 25 °C.

3.4. UV-visible studies

The stoichiometry of copper(II) complex **2** was studied in solution by using UV-visible titrations by using the mole ratio method. The spectra of BzTren with Cu(II) ion in aqueous methanol (33%, *v/v*) show a broad band at 679 nm and shoulder at 847 nm, which can be assigned to the A'→E" transition for a trigonal bipyrimal Cu(II) complex [22–24]. As seen in Fig. 3 (upper), the absorption intensity increases as a function of $[Cu^{2+}]/[BzTren]$ mole ratio. From the inflection point in the absorbance/mole ratio plots at values between 0.8 and 1.0, it can be inferred that 1:1 complex species are formed. The generation of BzTren-Cu(II)-bound hydroxo complex species was also investigated in solution by measuring the absorbance of complex **2** at different pH values in aqueous methanol (33%, *v/v*). As seen in Fig. 3 (lower), a new band gradually appeared at 679 nm upon increasing the pH value. This indicates that the geometry may distort from trigonal bipyramidal to a square pyramidal structure due to the formation of

$[BzTren\text{-}Cu(OH)]^{+}$ [25]. The absorbance indicates a sigmoidal change in the pH range 8.0 to 9.0, which corresponds to a change from $[BzTren\text{-}Cu(H_2O)]^{2+}$ to $[BzTren\text{-}Cu(OH)]^{+}$. From the fitting curve, the obtained pK_a value for the coordinated water molecule of complex **2** is *ca* 8.86, which in a good agreement with potentiometric titration data.

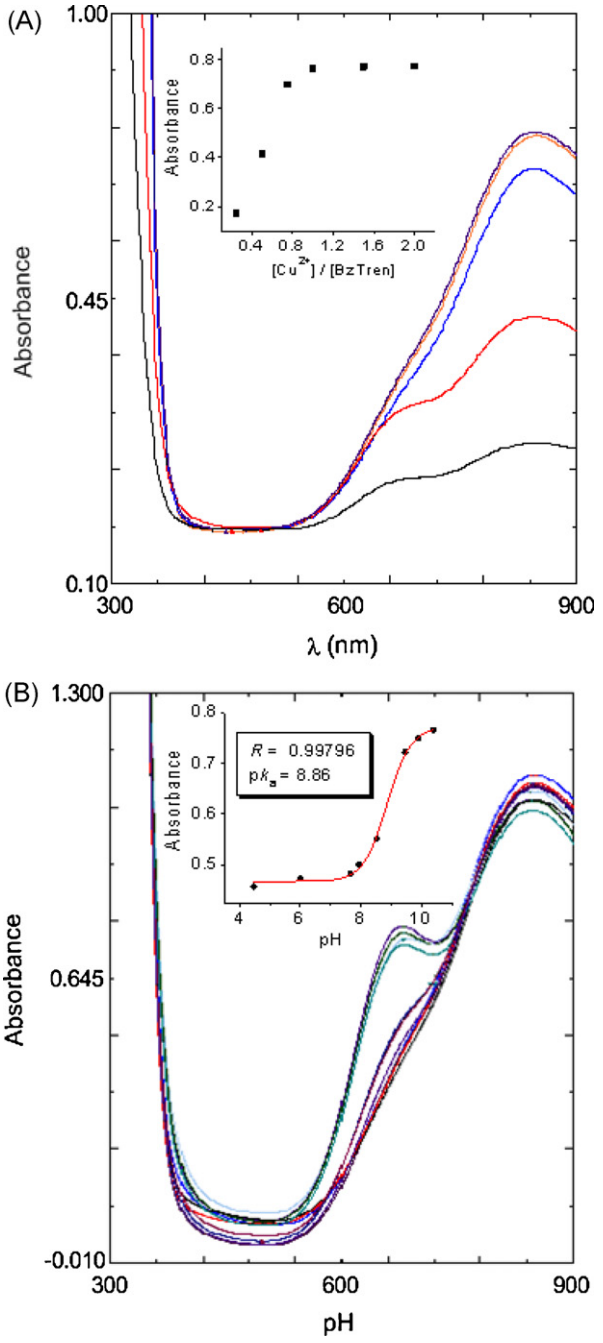

Fig. 3. Changes of UV-vis absorption of (A) the ligand BzTren (1.0×10^{-3} M) as a function of $[Cu^{2+}]$ at different ratios (0.25–1.50) in aqueous methanol (33%, *v*/*v*); (B) the copper complex **2** (1.0×10^{-3} M) as a function of pH (0.1 M $NaNO_3$, 25 ± 0.1 °C).

3.5. Electrochemical studies of the ligand BzTren and its zinc(II) and copper(II) complexes 1 and 2

The cyclic voltammogram of zinc(II) complex **1** (Supplementary material, S1) showed two couple redox

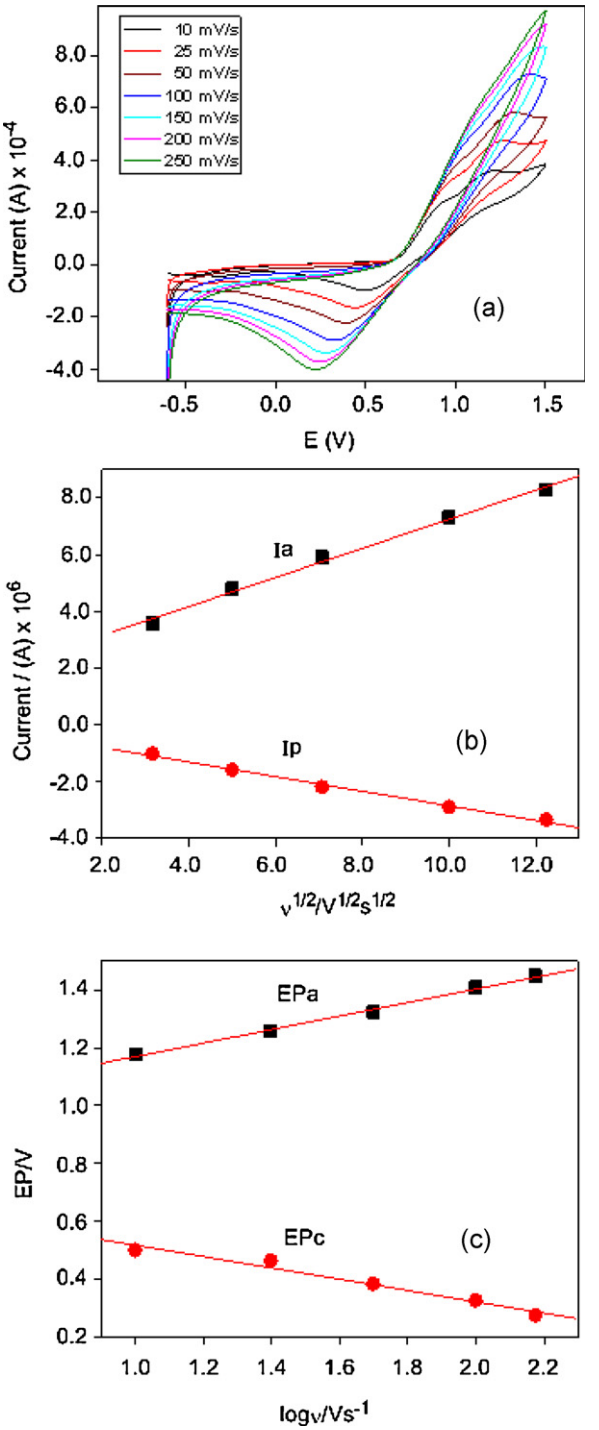

Fig. 4. The effect of scan rate on the voltammetric response of copper(II) complex **2** at 10, 50, 100, 150, 200 and 250 V/s using 0.1 M sodium sulphate containing 0.1 M potassium chloride (pH = 9) as a supporting electrolyte.

systems: two anodic peaks at 1.08 V (Epa1) and 1.4 V (Epa2) in the forward scan and another two cathodic peaks at 0.44 V (Epc1) and 1.02 V (Epc2) in the reverse scan. The peak separation potential ΔE = (Epa - Epc), between the first couple (Epa1 and Epa2) and second couple (Epc1 and Epc2) is 637 and 387 mV, respectively. The appearance of the two redox couples might support the formation of zinc(II) complex **1**. The higher peak separation potential between the two couples suggests that Zn(II)/Zn(I) and Zn(I)/Zn(0) redox couples are quasi-reversible behavior with a slow electron transfer. Their electrode reactions may be shown as follow [26]:

(a) Cathodic reaction:

$[BzTren\text{-}Zn(H_2O)]^{2+} + e^- \rightarrow [BzTren\text{-}Zn(H_2O)]^{+} + e^- \rightarrow [BzTren\text{-}Zn(H_2O)]$.

(b) Anodic reaction:

$[BzTren\text{-}Zn(H_2O)] - e^- \rightarrow [BzTren\text{-}Zn(H_2O)]^{+} - e^- \rightarrow [BzTren\text{-}Zn(H_2O)]^{2+}$.

The same behavior was obtained for Copper(II) complex **2**, where it also shows two anodic peaks in the forward scan (Epa1 at 1.04 V V/s, Epa2 at 1.34 V/s) and two cathodic peaks in the reverse scan (Epc1 at 0.42 V/s, Epc2 at 0.97 V/s). The peak separation potentials for the first and second couples are 620 and 370 mV, respectively. This large separation suggests that Cu(II)/Cu(I) and Cu(I)/Cu(0) redox couples are also quasi-reversible behavior [27].

The effect of scan rate on the peak potential was also investigated. A seen in Fig. 4a, by increasing the scan rate value, the anodic peak potential shifted to more positive value and the cathodic peak potential shifted to more negative values. The separation between the peak potentials, ΔE is a characteristic behavior for a quasi-reversible system [27]. Plotting the peak potential *versus* the logarithm of the scan rate values for both anodic and cathodic peaks showed two straight lines (Fig. 4b, c). The results showed that the linear regression equations were calculated as Epa (V) = 0.93639 + 0.23318 log ν (r = 0.9988) and Epc (V) = 0.71179 − 0.1954 log ν (r = 0.9923).

3.6. Thermal analysis

The thermal analysis indicates that the decomposition of the complexes proceeds in several stages. The temperature ranges, percentage mass losses, and the nature of each event of the decomposition reactions are given in Table 2 together with decomposed and residual species. The $[BzTren\text{-}Zn(OH_2)](NO_3)_2$ **1** decomposes in three stages. Typical TG-DTG-DSC curves of complex **1** are presented in Fig. 5. The big mass loss and broad peak are observed in the TG and DTG curves, respectively. The course of the DSC curve showed three endothermic peaks at 395, 592, and 802 K. Mass loss in the beginning of the second stage is slow and becomes rapid as decomposition proceeds. The first step is at 395 K; with a constant weight loss of 3.08% due the loss of the coordinated water molecule (Calc. 2.89%). The second step is at 592 K and is accompanied by a total mass loss of 61.29% due to the loss of $(Et_3N + 3\,C_6H_6 + 1.5\,N_2)$ (Calc. 60.70). The rest of the molecule decomposes in the third step leading to the formation of zinc carbide, ZnC_2 as final solid product (Found 13.80%; calc. 14.36%).

The pyrolysis of $[BzTren\text{-}Cu(OH_2)](NO_3)_2 \cdot H_2O$ **2** proceeds in four stages (Fig. 6). The first and second stages in the temperature range of 322–459 K achieve a total mass loss of 4.84% (calc. 5.14%) are due to the loss of two water molecules: one is related to the dehydration of the lattice water molecule and the other is related to the dehydration of the coordinated water molecule. The third step in the temperature range of 463–691 K (endothermic peak, DSC: 502) with a mass loss of 58.52% (calc. 60.81%) are attributed to the decomposition of the organic part of the complex. The final step is attributed to the decomposition of two nitrate groups (cal. 19.93%) to copper carbide, CuC_2 as final solid product (Found 14.34%; calc. 14.06%). Based on the DSC temperatures of the decomposition of complexes **1** and **2**. The thermal stabilities of the complexes depends on the central metal ions, which are

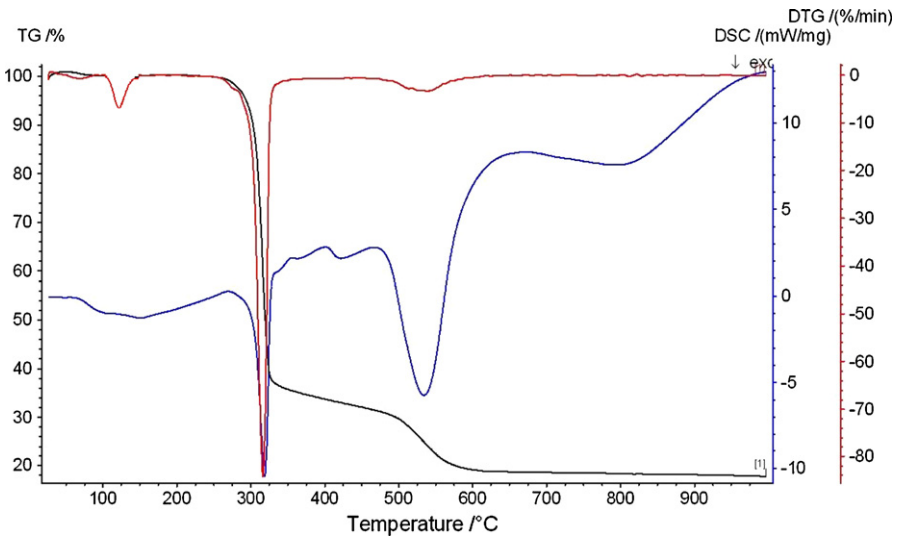

Fig. 5. TGA-DTG-DSC curves of complex **1** in the temperature ranges 30–1000 °C.

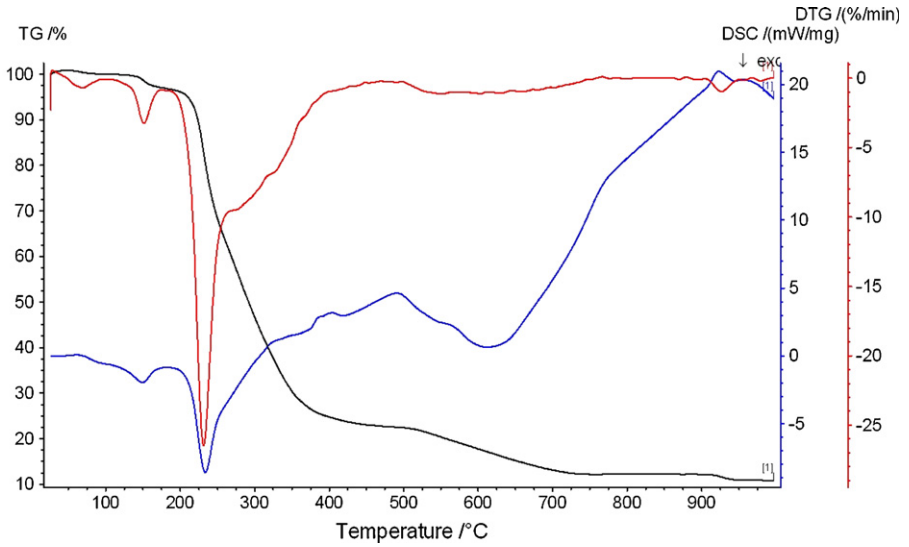

Fig. 6. TGA-DTG-DSC curves of complex **2** in the temperature ranges 30–1000 °C.

in the sequence of Cu^{2+} (884) > Zn^{2+} (808 K). In order to study the influence of metal ions interaction with the ligand BzTren. The stability of the obtained complexes **1** and **2** were investigated kinetically by using Coats-Redfern [28] eq. (1). The results are listed in Table 3. The calculation of the thermodynamic data were applied for the dehydration and the decomposition peaks of each complex.

$$\log\left[\frac{1-(1-\alpha)^{1-n}}{T^2(1-n)}\right] = \log\frac{AR}{qE_a}\left[1-\frac{2RT}{E_a}\right] - \frac{E_a}{2.3RT} \qquad (1)$$

where α is the fraction of the sample decomposed at time t, T is the derivative peak temperature (K), n is the order of reaction, A is the frequency factor, R the molar gas constant, E_a is the activation energy. A plot of $\log[-\log(1-\alpha)T^2]$ *versus* $1/T$ gives the slope for evaluation of the activation energy. The thermodynamic parameters, ΔH, ΔS, and ΔG were computed using the relationships [29]: $\Delta H = E - RT$, $\Delta S = R[\ln(Ah/kT)^{-1}]$, and $\Delta G = \Delta H - T\Delta S$. where k is Boltzmann's constant and h is Planck's constant. The higher values of activation energies for the dehydration of the water molecule indicate that they are coordinated to the metal. The relatively high values for the second decomposition step as well as the third and fourth decomposition steps indicate that the organic part of the ligand are strongly coordinated to the metal (II) ions. The negative values of entropies in the second and the other following steps indicate that the activated complex have more ordered structure than the reactants [30]. This also indicates that the copper(II) complex **2** has a higher thermal stabilities than complex **1**.

3.7. Kinetic studies for the hydrolysis reactions of parathion by using the model complexes 1 and 2

The hydrolysis reaction of parathion (DENTP) was examined using the model complexes **1** and **2**. The hydrolysis reactions were investigated in aqueous methanol (33%, *v/v*). Upon hydrolysis, DENTP decompose into *p*-nitrophenolate, NP^- and diethyl thiophosphate, $DETP^-$, respectively. The catalytic reactions were followed by an increase in absorption maximum at 400 nm for generation of *p*-nitrophenolate. The pH-dependence of the observed pseudo-first-order rate constants, k_{obs} studied over the pH range 7.0–10.5 are shown in Table 4 and Fig. 7. The copper(II) complex **2** was found to be more effective than zinc(II) complex **1** towards the hydrolysis of DENTP. This phenomenon may be due to the higher electrophilic character of copper(II) ion comparing to zinc(II) ion.

The pH-rate constant k_{obs} profiles for the hydrolysis reactions displayed sigmoidal curves with inflection points around the pK_a values of the coordinated water molecules

Table 3
Kinetic and thermodynamic data of complexes **1** and **2**.

Complex	Step	ΔE	ΔH	$\Delta\Sigma$	$\Delta\Gamma$	R
1	1	224	221.2	0.53	70.9	0.987
	2	278.5	275.6	−0.89	82.4	0.979
	3	9.6	86.6	−0.827	96.34	0.967
2	1	377	374.2	1.09	68.23	0.992
	2	247.7	244.8	0.586	74.7	0.989
	3	320.5	227.6	−0.59	77.13	0.991
	4	387.8	384.8	−0.79	84.6	0.977

Table 4
The observed pseudo-first-order rate constants, k_{obs} (s^{-1}) for the hydrolysis of parathion (DENTP) (4×10^{-5} M) catalyzed by using complexes **1** and **2** (1.0×10^{-3} M) at different pH values in aqueous MeOH (33%, *v*/*v*) at $I = 0.1$ M $NaNO_3$ and 50.0 ± 0.2 °C.

pH	[BzTren-Zn(H_2O)] **1** $k_{obs} \times 10^{-6}$	[BzTren-Cu(H_2O)] **2** $k_{obs} \times 10^{-6}$	Blank $k_{obs} \times 10^{-7}$
7.0	0.524	0.632	———
7.5	0.742	1.791	1.4981
8.0	0.938	4.970	3.0530
8.5	1.311	11.04	5.8703
9.0	2.040	17.22	8.7594
9.5	4.562	23.79	15.280
10	7.231	24.02	17.993
10.5	8.780	24.60	18.769
11.0	9.671	25.31	22.56

in complexes **1** and **2**. Such pH-rate profile was observed in a number of phosphate ester hydrolysis promoted by using copper(II) [31], cobalt(II) [32–35], and zinc(II) complexes [18–24] and are indicative of the involvement of metal-hydroxo species in the catalytic process. The pK_a values obtained from these inflection points are in good agreement with those obtained from pH, UV-visible, and ^{1}H NMR titrations. Therefore, the metal(II)-bound hydroxo species of these complexes are believed to be active catalyst for hydrolyzing the activated phosphate triester DENTP.

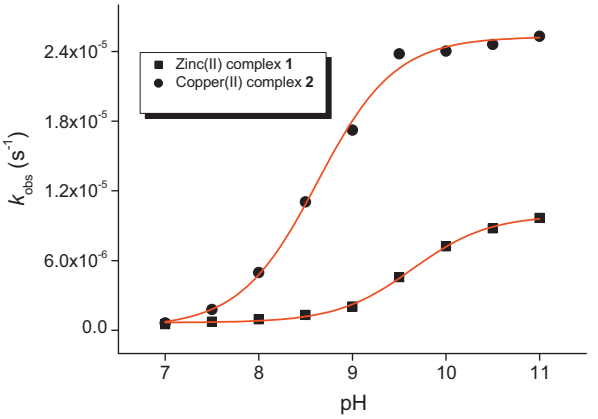

Fig. 7. Hydrolysis rate constant, k_{obs} of parathion (4×10^{-5} M) catalyzed by using complexes **1** and **2** (1.0×10^{-3} M) at different pH values in aqueous methanol (33%, *v*/*v*) at $I = 0.1$ M $NaNO_3$ and 50.0 ± 0.2 °C.

On the basis of the above-mentioned kinetic studies of the phosphate triester DENTP in aqueous methanol and the isolation of the aqua model complexes **1** and **2** and investigating their hydroxide derivatives as well as the formation of BzTren-Zn-bound diethyl thiophosphate **3**, we proposed a mechanism for the hydrolysis of DENTP (Scheme 3). At the first step, the coordinated water

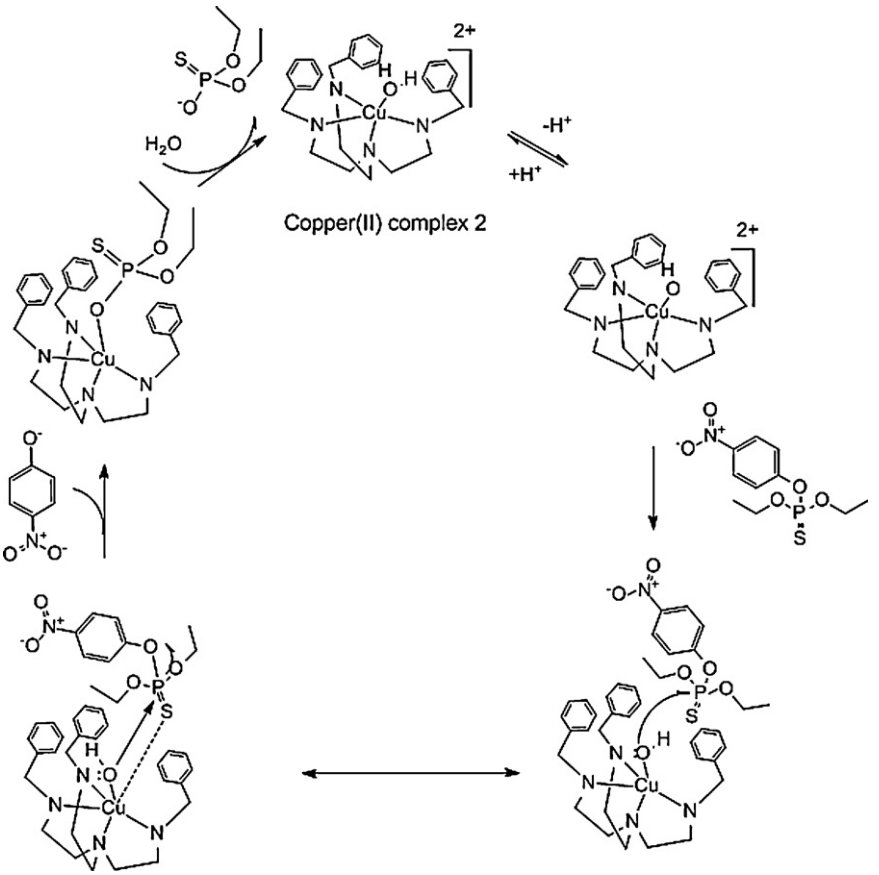

Scheme 3. Proposed mechanisms for the action of copper(II) complex **2** towards the hydrolysis of the toxic organophosphate parathion.

molecule in **1** and **2** can be deprotonated at pH between 8.0 and 9.5 to produce the metal(II)-bound hydroxo species [18,19]. Secondly, the metal center delivers the coordinated hydroxide which can nucleophically attack the toxic DENTP molecule, while the metal ion simultaneously withdraws electron density away from the phosphorus atom by interacting with the phosphoryl sulfur, forming penta-coordinated intermediate; finally, the *p*-nitrophenolate is released and the metal(II)-bound phosphate intermediate is replaced by water to form again the starting catalyst aqua metal(II) complexes, which are ready to start another catalytic cycle.

4. Conclusion

Two aqua metal(II) complexes $[BzTren\text{-}M(OH_2)]^{2+}$ **1** and **2** ($M^{2+} = Zn^{2+}$ and Cu^{2+}) derived from the tetradentate ligand tris(2-benzylaminoethyl)amine (BzTren) were synthesized and fully characterized by using FT-IR spectroscopy, elemental analysis, and thermal analysis. Solution studies of the metal–ligand interactions for determining the stoichiometry and the pK_a value of the coordinated water molecule using potentiometric, ^{1}H NMR and UV-visible titrations. The reactivity of these aqua model complexes as potential catalysts, especially the nature of metal ions on the hydrolysis of *O,O*-diethyl thiophosphate (DENTP) was investigated. The results showed that copper(II) complex **2** is more effective hydrolytic catalyst than complex **2**. This phenomenon may be due to the fact that copper(II) is likely to be more electron-withdrawing ion and has higher electrophilicity. Therefore, it can activate the nucleophile OH^- most effectively. Zinc(II) is the opposite and has the lowest activity.

Acknowledgements

This work was financially supported by Taif University, Saudi Arabia, Project No. 1/430/448.

Appendix A. Supplementary data

Supplementary data associated with this article can be found, in the online version, at doi:10.1016/j.crci.2011.10.012.

References

[1] (a) Y.C. Yang, J.A. Baker, J.R. Ward, Chem. Rev. 92 (1992) 1729;
(b) Y.C. Yang, Acc. Chem. Res. 32 (1999) 109.
[2] (a) J. Chin, X. Zou, J. Am. Chem. Soc. 106 (1984) 3687;
(b) N. Kitajima, S. Hikichi, M. Tanaka, Y. Moro-oka, J. Am. Chem. Soc. 115 (1993) 5496.
[3] (a) Zhang, R. Van Eldik, T. Koike, E. Kimura, Inorg. Chem. 32 (1993) 5749;
(b) A. Looney, R. Han, K. McNeill, G. Parkin, J. Am. Chem. Soc. 115 (1993) 4690;
(c) E. Kimura, I. Nakamura, T. Koike, M. Shionoya, Y. Kodama, T. Ikeda, M. Shiro, J. Am. Chem. Soc. 116 (1994) 4764;
(d) H. Adams, N.A. Bailey, D.E. Fenton, Q.Y. He, J. Chem. Soc. Dalton Trans. (1996) 2857.
[4] (a) T. Tanase, J.W. Yun, S.J. Lippard, Inorg. Chem. 35 (1996) 3585;
(b) J. Suh, S.J. Son, M.P. Suh, Inorg. Chem. 37 (1998) 4872.
[5] (a) K. Ogawa, K. Nakata, K. Ichikawa, Chem. Lett. (1998) 797;
(b) P.E. Jurek, A.E. Martell, Inorg. Chem. 38 (1999) 6003;
(c) P.E. Jurek, A.E. Martell, Inorg. Chim. Acta 287 (1999) 47.
[6] (a) K. Ichikawa, M.K. Uddin, K. Nakata, Chem. Lett. (1999) 115;
(b) H. Kurosaki, T. Tawada, S. Kawasoe, Y. Ohashi, M. Goto, Bioorg. Med. Chem. Lett. 10 (2000) 1333;
(c) T. Gajda, R. Kramer, A. Jancso, Eur. J. Inorg. Chem. (2000) 1635.
[7] (a) P. Woolley, Nature (London) 258 (1975) 677;
(b) P. Woolley, J. Chem. Soc. Perkin Trans. 2 (1977) 318.
[8] (a) S.H. Gellman, R. Peter, R. Breslow, J. Am. Chem. Soc. 108 (1986) 2388;
(b) J.T. Groves, R.R. Chambers, J. Am. Chem. Soc. 106 (1984) 630;
(c) B.L. Iverson, R.A. Lerner, Science 243 (1989) 1185.
[9] A.J. Vila, C.O. Fernandez, J. Am. Chem. Soc. 118 (1996) 7291.
[10] Y.R. Alsfaser, S. Trofimenko, A. Looney, G. Parkin, H. Vahrenkamp, Inorg. Chem. 30 (1991) 4098.
[11] L. Cronin, S.P. Foxon, P.J. Lusby, P.H. Walton, J. Biol. Inorg. Chem. 6 (2001) 367.
[12] P. Tecilla, U. Tonellato, A. Veronese, F. Felluga, P.J. Scrimin, J. Org. Chem. 62 (1997) 7621.
[13] R. Gregorzik, U. Hartmann, H. Vahrenkamp, Chem. Ber. 127 (1994) 2117.
[14] U. Hartmann, R. Gregorzik, H. Vahrenkamp, Chem. Ber. 127 (1994) 2123.
[15] R. Breslow, R. Smiley, T. Tarnowski, J. Am. Chem. Soc. 105 (1993) 5337.
[16] M.J. Hannon, P.C. Mayer, P.C. Taylor, Angew. Chem. Int. Ed. 40 (2001) 1081.
[17] M.M. Ibrahim, N. Shimomura, K. Ichikawa, M. Shiro, Inorg. Chim. Acta 313 (2001) 125.
[18] (a) M.M. Ibrahim, K. Ichikawa, M. Shiro, Inorg. Chim. Acta 353 (2003) 187;
(b) T. Echizen, M.M. Ibrahim, K. Nakata, M. Izumi, K. Ichikawa, M. Shiro, J. Inorg. Biochem. 98 (2004) 1347;
(c) M.M. Ibrahim, Inorg. Chem. Commun. 9 (2006) 1215;
(d) M.M. Ibrahim, G.A.M. Mersal, J. Inorg. Organomet. Polym. 19 (2009) 549;
(e) M.M. Ibrahim, J. Inorg. Organomet. Polym. 19 (2009) 532.
[19] Y. Makita, K. Sugimoto, K. Furuyoshi, K. Ikeda, S. Fujiwara, T. Shin-ike, A. Ogawa, Inorg. Chem. 49 (2010) 7220.
[20] R.G. Bates, M. Paabo, R.A. Robinson, J. Phys. Chem. 67 (1963) 1833.
[21] E.A. Martell, R.J. Motekaitis, The determination and use of stability constants, 2nd ed., VCH, New York, 1992, 143.
[22] (a) B.J. Hathaway, in: G. Wilkinson, R.D. Gillard, J.A. McCleverty (Eds.), Comprehensive Coordination Chemistry, vol. 5, Pergamon, Press, Oxford, England, 1987, 533 pp.;
(b) D. Kroczewska, B. Kurzak, J. Jezierska, Polyhedron 25 (2006) 678.
[23] (a) S.S. Massoud, et al. Eur. J. Inorg. Chem. (2008) 3709;
(b) D.H. Powell, A.E. Merbach, I. Fabian, S. Schindler, R. van Eldik, Inorg. Chem. 33 (1994) 4468.
[24] F. Thaler, C.D. Hubbard, F.W. Heinemann, R. van Eldik, S. Schindler, I. Fabian, A.M. Dittler-Kingemann, F.E. Hahn, C. Orvig, Inorg. Chem. 37 (1998) 4022.
[25] B.J. Hathway, J. Chem. Soc. Dalton Trans. (1972) 1196.
[26] S.S. Shammi, A.A. Shaikh, S.M.S. Islam, M.Q. Moreton, Malays. J. Chem. 10 (2008) 9.
[27] (a) S. Chandra, R. Kumar, R. Sigh, A.K. Jain, Spectrochimica Acta A 65 (2006) 582;
(b) S. Chandra, R. Kumar, Spectrochimica Acta A 62 (2005) 1050.
[28] (a) E. Laviron, J. Electroanal. Chem. 52 (1974) 355;
(b) E. Laviron, J. Electroanal. Chem. 101 (1979) 19.
[29] A.W. Coats, I.P. Redfern, Nature 201 (1964) 68.
[30] R.M. Mahfouz, M.A. Monshi, S.A. Alshehri, N.A. El-Salam, A.M.A. Zaid, Synth. React. Inorg. Met. Org. Chem. 31 (2001) 1873.
[31] T. Hatakeyama, Z. Liu, Handbook of thermal analysis, Wiely, Chichester, UK, 1998.
[32] Y. Fujii, T. Itoh, K. Onodera, T. Tada, Chem. Lett. (1995) 305.
[33] J.R. Morrow, W.C. Trogler, Inorg. Chem. 27 (1988) 3387.
[34] J. Burstyn, K.A. Deal, Inorg. Chem. 32 (1993) 3585.
[35] R.L. Fanshawe, A.G. Blackman, C.R. Clark, Inorg. Chim. Acta A 342 (2003) 114.